Cancer Therapy: Clinical

Clinical Cancer Research

Prospective Trial of Synchronous Bevacizumab, Erlotinib, and Concurrent Chemoradiation in Locally Advanced Head and Neck Cancer

David S. Yoo[1], John P. Kirkpatrick[1], Oana Craciunescu[1], Gloria Broadwater[3], Bercedis L. Peterson[3], Madeline D. Carroll[1], Robert Clough[1], James R. MacFall[2], Jenny Hoang[1,2], Richard L. Scher[4], Ramon M. Esclamado[4], Frank R. Dunphy[5], Neal E. Ready[5], and David M. Brizel[1,4]

Abstract

Purpose: We assessed the safety and efficacy of synchronous VEGF and epidermal growth factor receptor (EGFR) blockade with concurrent chemoradiation (CRT) in locally advanced head and neck cancer (HNC).

Experimental Design: Newly diagnosed patients with stage III/IV HNC received a 2-week lead-in of bevacizumab and/or erlotinib, followed by both agents with concurrent cisplatin and twice daily radiotherapy. Safety was assessed using Common Toxicity Criteria version 3.0. The primary efficacy endpoint was clinical complete response (CR) rate after CRT.

Results: Twenty-nine patients enrolled on study, with 27 completing therapy. Common grade III toxicities were mucositis ($n = 14$), dysphagia ($n = 8$), dehydration ($n = 7$), osteoradionecrosis ($n = 3$), and soft tissue necrosis ($n = 2$). Feeding tube placement was required in 79% but no patient remained dependent at 12-month posttreatment. Clinical CR after CRT was 96% [95% confidence interval (CI), 82%–100%]. Median follow-up was 46 months in survivors, with 3-year locoregional control and distant metastasis-free survival rates of 85% and 93%. Three-year estimated progression-free survival, disease-specific survival, and overall survival rates were 82%, 89%, and 86%, respectively. Dynamic contrast enhanced MRI (DCE-MRI) analysis showed that patients who had failed had lower baseline pretreatment median K^{trans} values, with subsequent increases after lead-in therapy and 1 week of CRT. Patients who did not fail had higher median K^{trans} values that decreased during therapy.

Conclusions: Dual VEGF/EGFR inhibition can be integrated with CRT in locally advanced HNC, with efficacy that compares favorably with historical controls albeit with an increased risk of osteoradionecrosis. Pretreatment and early DCE-MRI may prospectively identify patients at high risk of failure. *Clin Cancer Res; 18(5); 1404–14. ©2012 AACR.*

Introduction

Nearly 30,000 cases of locally advanced, nonmetastatic head and neck cancers (HNC) are diagnosed annually in the United States (1). The current nonsurgical standard of care for these patients is concurrent chemoradiation (CRT). A recent meta-analysis shows a 6.5% absolute survival benefit at 5 years for CRT compared with radiation therapy (RT) alone with the majority of benefit derived from improved locoregional control (LRC; ref. 2). Locoregional control and overall survival (OS) remain suboptimal despite these improvements, however.

The anatomically based tumor-node-metastasis (TNM) staging system provides prognostic information and guides management, but patients with similar disease stages often exhibit markedly different outcomes despite undergoing identical treatments. Worse prognosis in HNC, independent of TNM stage, has been correlated with differences in tumor oxygenation status (3). Hypoxia induces secretion of proangiogenic cytokines including VEGF, with downstream increases in vascular permeability and elevated interstitial fluid pressure (IFP; ref. 4). Overexpression of VEGF in HNC is correlated with higher metastatic potential and worse survival (5, 6). The anti-VEGF antibody bevacizumab has shown direct anti-vascular effects with enhanced radiosensitivity in both preclinical and clinical settings (7). A phase I study of recurrent/poor prognosis of patients with HNC integrated bevacizumab into an FHX (fluorouracil, hydroxyurea, radiation) CRT platform with favorable anti-tumor activity but higher-than-expected rates of fistula formation and tissue necrosis (8).

Authors' Affiliations: Departments of [1]Radiation Oncology and [2]Radiology, [3]Cancer Statistical Center, Department of Biostatistics and Bioinformatics, [4]Division of Otolaryngology, Department of Surgery, and [5]Division of Medical Oncology, Department of Medicine, Duke University Medical Center, Durham, North Carolina

Corresponding Author: David S. Yoo, Department of Radiation Oncology, Duke University Medical Center, Box 3085, Durham, NC 27710. Phone: 919-668-5637; Fax: 919-668-7345; E-mail: david.yoo@dm.duke.edu

doi: 10.1158/1078-0432.CCR-11-1982

Translational Relevance

The definitive, nonsurgical management of locally advanced nonmetastatic HNC has steadily evolved to the current standard-of-care concurrent chemotherapy and radiation. Despite technological advances in radiation delivery and recognition of patient populations (human papilloma virus) with improved prognosis, treatment failure remains a difficult dilemma with few salvage options. Molecular agents that target the VEGF and epidermal growth factor receptor (EGFR) pathways have already been incorporated into treatment regimens for recurrent/metastatic HNC with improved outcomes. This study represents the first to target both pathways in conjunction with a chemoradiation platform in patients with treatment-naïve, nonmetastatic HNC. Moreover, we examined the prognostic and predictive use of dynamic contrast enhanced MRI in this patient population.

Poorer outcomes in HNC have also been associated with overexpression of the epidermal growth factor receptor (EGFR; ref. 9). The addition of the anti-EGFR antibody cetuximab to definitive RT improved locoregional control and OS in patients with locally advanced HNC compared with RT alone (10). In the recurrent/metastatic setting, EGFR blockade with monoclonal antibody or small-molecule tyrosine kinase inhibitors, such as erlotinib or gefitinib, showed modest response rates in the 5% to 15% range, either as monotherapy or combined with platinum chemotherapy (11, 12).

Resistance to anti-EGFR therapy may result from alternate upregulation of VEGF-mediated pathways and increased angiogenesis (13). Dual inhibition of both EGFR and VEGF signaling cascades showed supra-additive antitumor effects in preclinical models (14). In recurrent/metastatic HNC, the combination of erlotinib and bevacizumab was well tolerated and showed a response rate of 15%, with prolonged benefit in a small subset of patients (15).

Increasing use of investigational/U.S. Food and Drug Administration (FDA)-approved agents that molecularly target the tumor microenvironment has magnified the need for robust correlative tools to identify novel physiologic and biologic factors that augment TNM staging. Dynamic contrast enhanced MRI (DCE-MRI) can provide data on perfusion, vascular permeability, and the proportion of tumor comprised by the interstitial space (16). DCE-MRI parameters have been correlated with tumor oxygenation status, microvessel density, and VEGF expression (17–19). DCE-MRI has been used to monitor changes in vascular permeability following treatment with bevacizumab (20). DCE-MRI parameters have also been correlated with local control, disease-free survival, and OS in multiple tumor sites, including HNC (21).

This prospective study examined the safety and efficacy of delivering bevacizumab and erlotinib in conjunction with CRT in patients with locally advanced nonmetastatic HNC. Serial DCE-MRI scans were also conducted before, during, and after treatment to characterize the effects of treatment on the tumor microcirculation and to generate preliminary data on the prognostic and predictive value of functional metabolic imaging (FMI) in this patient population.

Patients and Methods

Patient selection

Eligibility criteria included patients $\geq$18 years of age with newly diagnosed, previously untreated locally advanced head and neck squamous cell carcinoma with Karnofsky performance status $\geq$60 undergoing definitive curative-intent CRT. Postoperative patients were ineligible. Initial multidisciplinary evaluation included history and physical examination, fiberoptic endoscopy, examination under anesthesia with direct laryngoscopy, computerized tomography (CT) or MRI, chest radiograph, and combined positron emission tomography with CT. Tumors were staged according to American Joint Committee on Cancer 6th edition criteria. Patients with stage III/IV without distant metastatic disease were eligible. Patients with T1N1-2 disease or tumor encasement of the carotid artery were excluded. Other exclusion criteria are described in the legend of Fig. 1. Carotid ultrasound scans were conducted at initial screening and 1 month after CRT completion. Written informed consent was obtained on all patients prior to enrollment.

Study design

This trial was an investigator-initiated, open-label, nonrandomized single-institution study (clinicaltrials.gov: NCT00140556) conducted under the FDA Investigational New Drug (IND) program (IND #12451) with approval for enrollment of up to 30 patients. The study was also approved by the Duke Cancer Center Protocol Review Committee and Institutional Review Board of Duke University Health System (Durham, NC). The protocol schema is described in Fig. 1. In the lead-in phase, patients were randomly allocated to receive (i) 10 mg/kg bevacizumab on days 14 and 0; (ii) 100 mg erlotinib daily; or (iii) both agents. These separate cohorts were designed to facilitate correlative studies that examined the physiologic changes in treatment-naïve tumors induced by single versus dual biologic targeted therapy independent from another and separate from those induced by CRT. The reduced 100-mg erlotinib dose was chosen for additional safety, as both agents had not been previously combined in the CRT setting.

In the CRT phase, all patients received both targeted agents with cisplatin (CDDP) and twice daily 1.25 Gy intensity-modulated RT Monday–Friday with a 6-hour interfraction interval to 70 Gy. A scheduled 1-week treatment break was taken during week 4. CDDP was administered at 33 mg/m^2 on days 1 to 3 during weeks 1 and 5 of RT. Bevacizumab (10 mg/kg) was given on day 1 of RT and repeated every 14 days for 4 doses. Erlotinib (100 mg) was taken daily during RT except on days of CDDP

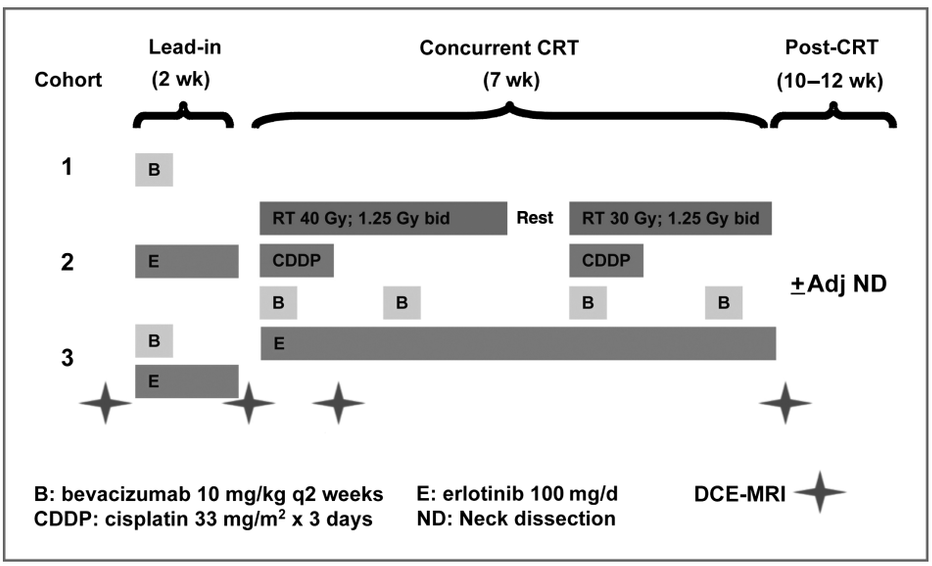

Figure 1. Protocol schema showing initial 2-week lead-in phase of molecular target agent(s), followed by 7-week concurrent CRT regimen with synchronous bevacizumab and erlotinib administration. The timing of the DCE-MRI scans is also indicated. Additional protocol exclusion criteria included history of malignancy other than basal cell skin cancer, history of claudication, bleeding, or thromboembolic disorders, blood pressure of >150/100 mm Hg, unstable angina, NYHA grade II or greater congestive heart failure, history of myocardial infarction or stroke within 6 months, major surgical procedure, open biopsy, or significant traumatic injury within 28 days prior to start of therapy, minor surgical procedures within 7 days prior to start of therapy, pregnancy or lactation, urine protein:creatinine ratio > 1.0 at screening, history of abdominal fistula, gastrointestinal perforation, or intra-abdominal abscess within 6 months, serious nonhealing wound, ulcer, or bone fracture, aspartate aminotransferase (AST), alanine aminotransferase (ALT), bilirubin, prothrombin time (PT) or partial thromboplastin time (PTT) >1.5× normal, platelets > 100,000, white blood cell (WBC) < 2,000, Hb < 10, creatinine clearance < 60 mL/h, or refusal to provide written informed consent.

administration. Adjuvant neck dissection was conducted 10 to 12 weeks posttherapy in N2 patients with clinical or radiographic evidence of residual disease and all N3 patients irrespective of response.

Statistical design

The primary objective of the study included safety and efficacy endpoints, monitoring both the ability to complete treatment and the clinical complete response (CR) rate at the primary site (or nodal sites for unknown primary patients) within 30 days of therapy completion. This conservative time point was chosen to identify persistent disease and trigger stopping rules as soon as possible. Target accrual was 28 patients, 2 of whom were expected to be unavailable for response evaluation. A Simon 2-stage optimal design with 1-sided α of 0.10 and power of 0.91 was used to test null and alternative hypotheses such that the ability to complete treatment and the primary site CR rate was <70% and >90%, respectively. Only if 23 (82%) or more of the 28 patients achieved these outcomes would the null hypothesis be rejected. The first stage of the design required at least 7 of the first 9 patients to complete treatment and achieve CRs to continue accrual.

Secondary endpoints of LRC, distant metastasis-free survival (DMFS), disease-specific survival (DSS), progression-free survival (PFS), and OS were defined from time on-study and estimated using the Kaplan–Meier method. The analysis of LRC included only locoregional recurrences as events; other failures were censored. DMFS was defined analogously. PFS included all failures as events except for death not due to disease, which was censored. DSS included disease-related deaths as events; other deaths were censored. OS included deaths due to any cause. Safety was assessed through collection of adverse events and laboratory tests based on Common Toxicity Criteria (CTC) version 3.0. Toxicity assessments were conducted weekly during treatment and posttreatment at 1 month and every 3 months through year 2.

DCE-MRI scanning

Imaging protocol. An initial pretreatment DCE-MRI (baseline) was conducted. Patients received 2 weeks of lead-in targeted therapy, followed by a second MRI (lead-in) prior to initiation of CRT. A third scan (week 1) was conducted after completion of the first week of CRT and synchronous targeted therapy. The fourth scan (end) was conducted at CRT completion. Ultimately, this final scan was discontinued (see Results). Serum banking was conducted with each DCE-MRI study for future correlative analyses.

DCE-MRIs were acquired on a 1.5T scanner (Signa Excite, GE Medical Systems, software version 11x and 14xm5) prior to and following a single bolus injection of 0.1 mmol/kg of gadolinium-DTPA using a dynamic coronal 3-dimensional (3D) fGRE sequence (fast gradient echo) with the following parameters: repetition time (TR) = 6.4 ms, echo time (TE) = 2 ms, field of view (FOV) = 24

$\times$ 24 cm^2, acquisition matrix size: 238 $\times$ 128, single scan duration = 10 s, number of scans = 31–33, 10-mm slice thickness using ZIP4 (48 slices; ZIP is a function available on GE scanners that improves through plane resolution by interpolating the acquired scan data to create new images), flip angle = 60 degrees. The final size of each voxel per scan was 10 mm^3. Imaging was done using the Linear Receive Anterior Neck Coil (GE Healthcare), with no head and neck immobilization device specific to radiation treatments. Additional MR series, namely T1-weighted coronal fast spin echo (FSE) series were acquired consecutively before and after contrast administration, which provided better anatomic spatial resolution. In addition, before contrast, 3D fGRE sequences were acquired at variable flip angles (VFA) = 10 and 45 degrees. These sequences were used to calculate the tissue T_{10} values pre-contrast agent administration (T_{10}) using the VFA method (22).

Scans were obtained in the axial plane at the beginning of the trial, but difficulties distinguishing the boundaries between tumor volumes and immediately adjacent major salivary glands and/or major blood vessels mandated a change in strategy. Thereafter, image acquisition was conducted in the coronal plane. Primary tumor and lymph node gross tumor volumes (GTV) were analyzed separately. Regions of interest were defined as the entire GTV as delineated by a radiation oncologist (D.M. Brizel or D.S. Yoo) and a radiologist (J. Hoang) on either an early subtraction map or on the post-contrast FSE T1 images.

Image processing. Monitoring of the temporal "wash in–wash out" of the contrast agent measures the vascular transfer constant (K^{trans}), which provides an estimate of vascular permeability, and the rate constant (K^{ep}). The extracellular, extravascular volume fraction (V^e) is described by the Tofts pharmacokinetic model ($V^e = K^{trans}/K^{ep}$; ref. 16). K^{trans} approximates perfusion in high permeability states such as untreated tumor (16). The images were analyzed using post-processing software from iCAD, Inc. that uses All Time Point (ATP) pharmacokinetic image analysis (23). All applicable parameters and settings of the MRI examination were used to fit voxel enhancement curves to the appropriate formula for estimation of tissue parameters. A detailed description of the procedure is published elsewhere (22).

Data analysis. The distribution of K^{trans} values for each patient was summarized by calculating its 25th and 75th percentiles and each 10th percentile from the 10th to 90th percentiles (total 11 percentiles). Data were grouped according to whether they were obtained from primary tumor or lymph nodes. Comparisons were then conducted within each group on the basis of whether or not a patient relapsed. The medians of each of the 11 percentiles were calculated and displayed with dot plots in which the x-axis represents the median K^{trans} value for a given percentile and the y-axis is labeled with the names of the 11 percentiles. Box and whisker plots were used to provide additional summary statistics describing the patient-specific distribution of the 50th percentile of K^{trans}. All analyses are descriptive rather than inferential because of the small sample size.

Results

Patient characteristics

Twenty-nine patients were enrolled from October 2005 to April 2009. One patient withdrew before starting treatment. A second patient withdrew during therapy due to acute toxicity but is included in the analyses. For the lead-in phase, 8 patients were allocated to the bevacizumab-alone cohort, 10 received erlotinib, and 10 received both agents. Table 1 describes patient and tumor characteristics. Eighty-two percent were T3/T4 and 79% had N2/3 disease. Mean gross primary and nodal GTVs were 46 and 24 cc, respectively. Human papilloma virus (HPV) status was available in 15 patients (2 cervical nodes, 3 oral tongue, and 10 oropharynx) by *in situ* hybridization and/or p16 immunohistochemistry. Ten (67%) tested positive for HPV (1 cervical node and 9 oropharynx). Of the 9 HPV-positive oropharynx patients, 8 had a history of tobacco use. In the 10 oropharynx patients without HPV data, 6 had used tobacco.

Treatment delivery

Median dose was 70 Gy (range, 69.5–71.5 Gy), and median treatment time was 44 days (range, 40–53 days). Twenty-six patients (93%) received the planned 2 cycles of concurrent cisplatin. The median bevacizumab dose was 3,905 mg (89.5% planned). Median erlotinib dose was 4,900 mg (97% planned).

Toxicity

Table 2 shows the incidence and severity of acute and chronic toxicities. One patient withdrew from protocol due to mucositis-related pain but completed CRT without treatment break. Thirteen patients required inpatient hospitalization, primarily for feeding tube placement and pain control secondary to mucositis. One patient in the erlotinib-alone cohort required temporary intensive care support after development of global myocardial ischemia resulting in pulmonary edema and shock liver, both of which were transient. She received less than 50% of the planned doses of both bevacizumab and erlotinib.

Overall, 26 patients (93%) developed some degree of oropharyngeal mucositis. Grade III mucositis occurred in 14 patients (50%), whereas grade III dysphagia developed in 8 patients (29%). Percutaneous feeding tubes were required prior to therapy in 4 patients. During protocol treatment, an additional 18 patients underwent placement of a nasogastric feeding tube. However, by 12 months posttherapy, no patient was feeding tube dependent.

Grade III osteoradionecrosis developed in 3 patients (11%), two with T3 tonsil primaries and one with unknown primary. One patient received both bevacizumab and erlotinib during lead-in but discontinued both (per request) during CRT after the scheduled treatment

Table 1. Patient and tumor characteristics

Characteristics	Patients, *n* (%)
Sex	
Male	22 (79)
Female	6 (21)
Age, y	
Median	53
Range	39–76
Race	
White	20 (71)
Black	5 (18)
Hispanic	1 (4)
Asian	2 (7)
Tobacco history	
Yes	18 (64)
No	10 (36)
Alcohol history	
Yes	14 (50)
No	14 (50)
Feeding tube present baseline	
Yes	4 (14)
No	24 (86)
Tumor site	
Tonsil	11 (39)
Base of tongue	8 (29)
Soft palate	1 (4)
Oral tongue	3 (11)
Oral cavity	1 (4)
Supraglottic larynx	1 (4)
Nasopharynx	1 (4)
Unknown primary	2 (7)
Stage	
III	3 (11)
IVA	21 (75)
IVB	4 (14)
Primary tumor volume, cc	
Mean	46.2
Range	3.3–211.2
Nodal tumor volume, cc	
Mean	23.8
Range	1.0–157.6

Table 2. Acute and late toxicities

	Grade II	Grade III	Grade IV
Acute toxicity			
Thrombocytopenia	0	0	2
Transaminitis	1	0	1
Mucositis	12	14	0
Dysphagia	5	8	0
Dehydration	11	7	0
Febrile neutropenia	0	5	0
Nausea/vomiting	23	4	0
Diarrhea	1	4	0
Drug-induced rash	13	2	0
Radiation dermatitis	8	2	0
Pneumonitis	0	2	0
Candidiasis	16	1	0
Fatigue	8	1	0
Hiccups	2	1	0
Anorexia	1	1	0
Cardiac ischemia	0	1	0
Hypokalemia	0	1	0
Hypotension	0	1	0
Vasculitis	0	1	0
Weight loss	15	0	0
Fever	5	0	0
Hypertension	4	0	0
Constipation	2	0	0
Elevated creatinine	1	0	0
Proteinuria	1	0	0
Tinnitus	1	0	0
	Grade I	**Grade II**	**Grade III**
Late toxicity			
Osteoradionecrosis	0	1	3
Soft tissue necrosis	0	0	2
Infection	0	3	1
Fibrosis	2	1	1
Parotiditis	0	0	1
Aspiration pneumonia	0	0	1
Xerostomia	6	2	0
Dysphagia	0	1	0

break, ultimately receiving 60% of the total planned doses of both agents. The other 2 patients were in the bevacizumab-alone lead-in cohort and had received all planned doses of bevacizumab but only 41% and 85% of erlotinib during CRT. Soft tissue necrosis developed in 2 oropharynx patients. One patient in the erlotinib-alone cohort healed after antibiotics alone. The second patient in the combined lead-in cohort underwent adjuvant modified neck dissection followed by pectoralis muscle flap reconstruction for postoperative chyle leak and subsequently developed an orocutaneous fistula that healed after hyperbaric oxygen therapy without the need for further surgical repair.

Efficacy

Primary site (or nodal sites for unknown primary patients) clinical CR was achieved in 27 of 28 patients [96%; 95% confidence interval (CI), 82%–100%]. Of the 23 patients with pretreatment nodal metastases, 17 (74%) had clinical CRs. Adjuvant neck dissections were conducted in 11 patients (5 CRs and 6 PRs), with residual nodal disease found in 4 of the partial responders.

Median follow-up for surviving patients was 46 months (range, 25–63 months). Five patients had documented disease progression posttreatment: 2 with local-only, 1 regional only, 1 regional plus distant metastasis, and 1 with distant-only failure. All of them have died. One additional

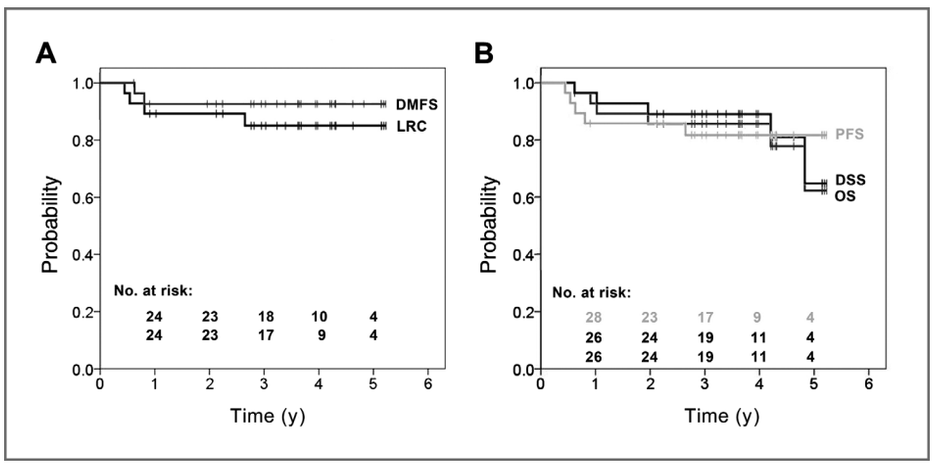

Figure 2. Kaplan–Meier curves for (A) locoregional control and DMFS and (B) DSS, PFS, and OS for all patients.

patient died of unknown cause without evidence of disease or treatment-related toxicity 6 months after completion of CRT and neck dissection. No other patient has died. At 3 years, LRC and DMFS rates were 85% (95% CI, 65%–94%) and 93% (95% CI, 74%–98%), respectively (Fig. 2A). Three-year DSS, PFS, and OS rates were 89% (95% CI, 70%–96%), 82% (95% CI, 62%–92%), and 86% (95% CI, 66%–94%), respectively (Fig. 2B).

DCE-MRI

The original protocol design included 4 DCE-MRI scans per patient. However, because of the high clinical CR rates, very few patients had lesions that could be visualized radiographically at treatment completion. Consequently, a protocol amendment deleted the fourth scan. Baseline, lead-in, and week 1 scans were conducted in 26, 24, and 24 patients, respectively. The first 6 patients were scanned in the axial plane; the others were imaged in the coronal plane. The median (25%–75% range) of the pretreatment primary tumor GTV was 41.4 cm^3 (14–66 cm^3), and the median pretreatment nodal GTV was 12.8 cm^3 (8–31 cm^3). Thus, the median number of voxels scanned per primary tumor and nodal GTV was 4,140 (1,400–6,600) and 1,280 (800–3,100), respectively.

Five of the 26 patients with baseline DCE-MRI studies recurred, all within 2 years of treatment completion. Their scans were compared with those from patients who remained disease-free. The distributions of patient-specific 50th percentile K^{trans} values for primary tumors and lymph nodes, respectively, for each of the 3 scanning time points are displayed in Fig. 3A and B.

Overall, both primary tumors and lymph nodes showed higher baseline K^{trans} values for patients who did not recur than for those who did. Moreover, K^{trans} values diminished in the early phases of treatment for patients who remained disease-free whereas they increased in those who recurred. The median of 50th percentile K^{trans} values obtained from primary tumors in patients who did not recur was 4.90 min^{-1} at baseline. K^{trans} decreased to 3.77 at the end of lead-in therapy and to 2.55 at week 1 of CRT. The median of 50th percentile K^{trans} values obtained from primary tumors in patients who recurred after treatment was 4.72 at baseline, increased to 5.74 after lead-in, and 5.77 at week 1 of CRT. Dot plots present the medians of all 11 percentiles of K^{trans} values from primary tumors in patients who did not recur (Fig. 4A) and those who did recur (Fig. 4B) from the serial scans obtained before and during treatment.

K^{trans} values obtained from lymph nodes showed similar patterns. In patients without recurrence, the median of 50th percentile K^{trans} values was 7.56 at baseline and decreased to 5.8 and 2.43 at lead-in and week 1 time points, respectively (Fig. 4C). For patients who recurred, the median of 50th percentile K^{trans} values was 4.43 at baseline and increased to 5.61 at lead-in and 6.55 at week 1 (Fig. 4D).

Discussion

This study represents the first to integrate synchronous multiagent molecular targeted therapy with curative-intent cisplatin-based CRT in locally advanced, nonmetastatic HNC. The results suggest that the combination of 10 mg/kg bevacizumab every 2 weeks and 100 mg erlotinib daily can be incorporated into a CRT platform.

Overall, treatment was feasible, with one patient not completing protocol-specified therapy. No on-treatment or treatment-related deaths were noted. The incidence of mucositis seen in the study (93% all grades, 50% grade III) is consistent with historical rates for altered fractionation RT (56% grade III-IV), as well as those prospectively reported with concomitant RT and cetuximab (93% all grades, 60% grade III-IV; refs. 10, 24). Of note, the study design incorporated a 1-week treatment break because of concern for potential excess mucositis with treatment intensification, perhaps explaining the lower rates of grade III mucositis seen. Still, for 22 patients (79%) who required nasogastric feeding tube placement at some point and had World Health Organization (WHO) toxicity criteria been used instead of CTC, the incidence of grade III-IV mucositis would have been higher. Importantly, no patient was feeding tube dependent at 12 months, which compares favorably with the 83% (anytime) and 41% (12 months) feeding tube rates reported in RTOG 99-14, a phase II study of concurrent cisplatin

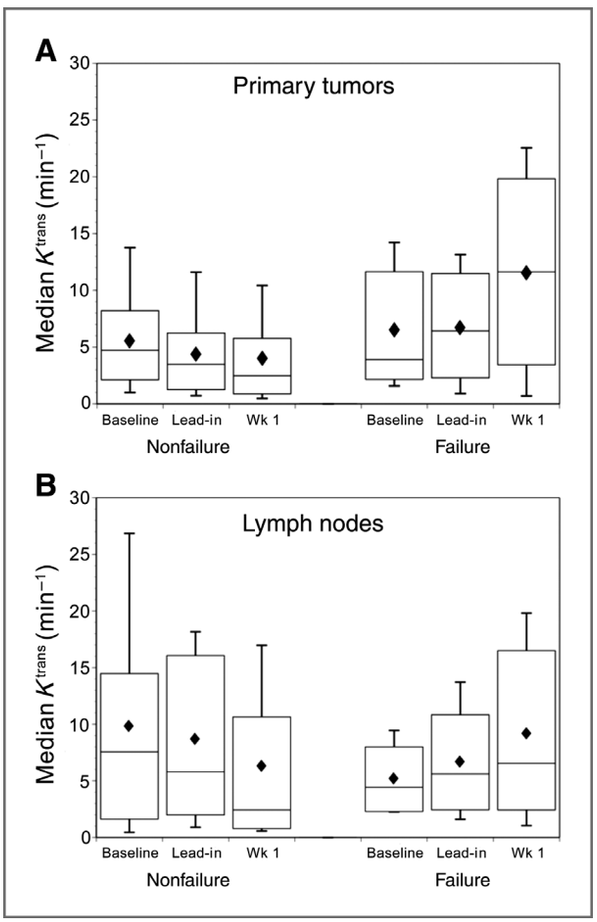

Figure 3. Box and whisker plot of the distribution of the 50th percentile of K^{trans} values in (A) primary tumors and (B) lymph nodes at baseline, after lead-in targeted therapy, and after week 1 of synchronous CRT and targeted therapy. Each set of plots is grouped by clinical outcome. The horizontal lines show the median and the diamonds show the mean. The 25th and 75th percentiles are defined by the upper and lower boundaries of the boxes. The vertical lines illustrate the 10th and 90th percentiles.

with accelerated RT in patients with locally advanced HNC (25).

The use of bevacizumab has been associated with severe bleeding events and poor wound healing. The current study had 5 patients (18%) develop grade III osteoradionecrosis or soft tissue necrosis, although 3 of them had not received full doses of both targeted agents. In a study of 43 patients with recurrent/poor-prognosis HNC, bevacizumab added to FHX CRT resulted in a 21% rate of ulceration/tissue necrosis or fistulas (8). Two thirds of their study population had received prior irradiation. A subsequent phase II study comparing FHX versus FHX plus bevacizumab in stage II-III and select patients with T4N0-1 HNC had 3 patients (16%) in the experimental arm requiring multiple surgeries for poor wound healing (26). Whether these rates would be lower in the setting of conventional once daily RT or with different concurrent chemotherapy agents is unknown and warrants further investigation in the context of clinical trials.

The current trial used a modified twice daily hyperfractionated regimen, which, at the time of its inception, had been shown to be superior to hyperfractionated RT alone in a randomized study (27). RTOG 0129, which compared concomitant boost accelerated fractionation CRT against standard once daily fractionation CRT, has subsequently reported no differences in toxicity or efficacy between the 2 arms (28). The optimal RT fractionation regimen to use with molecularly targeted agents is not established. In the pivotal cetuximab trial, unplanned subset analyses suggested that the survival benefit was seen in patients treated with twice daily or concomitant boost RT (10). The concomitant boost platform was chosen by the RTOG for its 0522 trial, which compared CRT versus CRT plus single-agent cetuximab. Preliminary results showed higher rates of mucositis and skin toxicity but no improvements in PFS or OS (29).

The addition of single-agent bevacizumab to CRT in patients with treatment-naïve nonmetastatic HNC was examined by Salama and colleagues as described earlier (26). The study was terminated early after 26 patients, due to unexpected locoregional progression in 4 of 5 T4N0-1 patients treated with bevacizumab and FHX. All 4 failures had unfavorable primary sites (2 oral cavity, 1 pyriform sinus, and 1 larynx). As their excellent results with FHX alone suggest, treatment intensification with bevacizumab may not be necessary in patients with intermediate-stage HNC. With only 2 T4N0-1 patients treated with FHX prior to early termination, the study appears too small to assess the efficacy of the combined regimen in more advanced disease.

Poor outcomes or resistance with single-agent molecular therapy have spurred interest in strategies that synchronously target multiple signaling pathways (30). Cohen and colleagues examined dual inhibition with erlotinib and bevacizumab in recurrent/metastatic HNC (15). The combination was well tolerated with a response rate of 15% and median PFS and OS durations of 4.1 and 7.1 months, respectively. However, coadministration has not always led to improved outcomes. The dual use of bevacizumab and erlotinib proved disappointing, with an estimated median time to progression of 40 days and median survival of 102 days in patients with gemcitabine-refractory pancreatic cancer (31). Even worse, the addition of cetuximab to bevacizumab and chemotherapy in first-line treatment of metastatic colon cancer resulted in shorter PFS and poorer quality of life compared with bevacizumab and chemotherapy alone (32).

The use of dual inhibition in conjunction with CRT in the present study showed 3-year LRC and OS rates of 85% and 86%, comparing favorably with historical outcomes for locally advanced HNC. Comparisons among different studies are challenging, given different eras and patient populations. Concurrent RT and cetuximab in the Bonner study showed 3-year LRC and OS rates of 47% and 55% (10). The concomitant boost CRT arm of RTOG 0129 showed 3-year LRC and OS rates of 71.8% and 70.3% (28). Two-year PFS and OS rates were 63% and 83% with CRT plus cetuximab in RTOG 0522 (29).

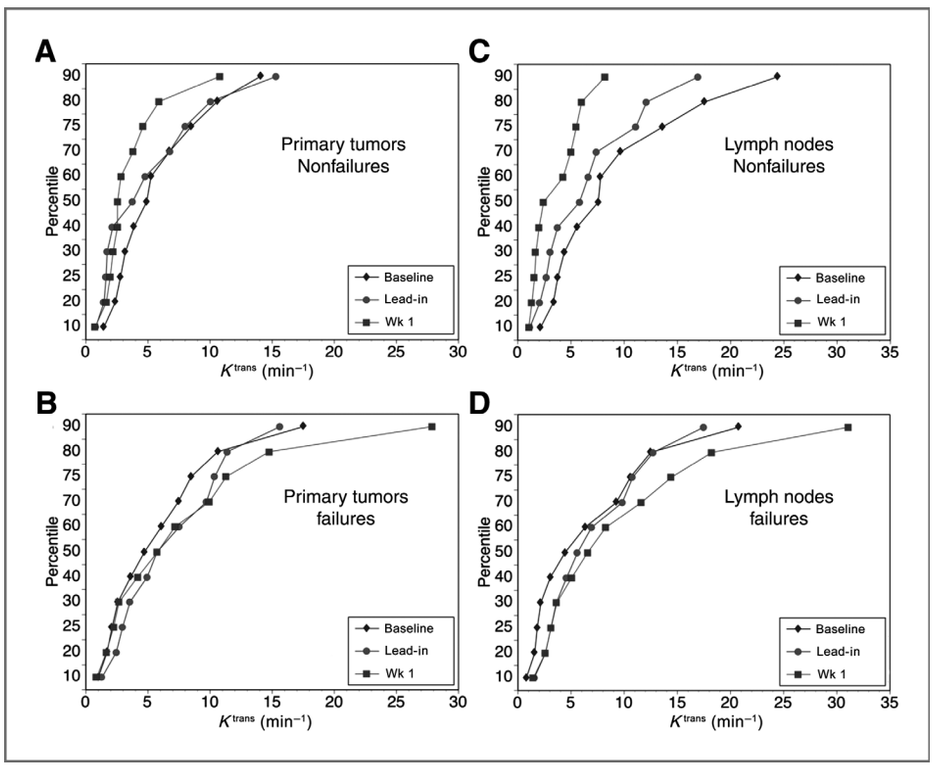

Figure 4. Dot plots of the medians of all 11 percentiles of K^{trans} values for the same time points as in Fig. 3. Data from patients who did not fail are shown in A (primary tumors) and C (lymph nodes). B (primary tumors) and D (lymph nodes) show the values for patients who did fail. K^{trans} decreases during the early phases of treatment in both the primary tumor and lymph nodes in patients who do not recur and increases in those who do recur.

As treatment strategies evolve, improved patient selection will be critical to identify those patients who may benefit most from therapeutic intensification. Retrospective review of RTOG 0129 found that HPV status strongly correlated with survival in oropharyngeal cancers, with 82% 3-year OS rate for HPV-positive versus 57% for HPV-negative patients (28). Further analysis suggested that patients could be subdivided into low-, intermediate-, and high-risk groups for death based on HPV status, tobacco history, tumor stage, and nodal stage. Given that a majority of our study patients were smokers with large T3/T4 tumors and N2/3 disease, it is less likely that HPV status accounted for the encouraging outcomes seen. Of the 5 patients who progressed, HPV was positive in one (base of tongue primary, local only), negative in one (occult primary, regional and distant), and unknown in the remaining 3 (soft palate, regional-only; oral cavity, local-only; nasopharynx, distant-only).

Potential correlative biomarkers in HNC remain elusive. *KRAS* mutation status appears to predict tumor response to cetuximab in metastatic colon cancer but not in HNC (33). While high *EGFR* gene copy number was associated with worse survival in patients treated with gefitinib, EGFR expression did not predict for response to erlotinib in heavily pretreated recurrent/metastatic patients (34, 35). Seiwert and colleagues showed that baseline VEGF plasma levels were neither prognostic nor predictive for response to bevacizumab (8). Changes in the tumor microenvironment, both by RT or molecularly targeted agents, can be monitored with FMI modalities such as DCE-MRI. FMI-derived data can potentially improve the *a priori* identification of patients at highest risk for failure and who might benefit most from therapeutic intensification, especially among heavy smokers with advanced HPV-negative disease. For these patients, treatment strategies that incorporate synchronous inhibition of multiple signaling pathways, induction chemotherapy regimens, and/or planned surgical resection may ultimately yield improved outcomes compared with CRT alone.

Conversely, FMI could facilitate the identification of patients who do NOT require more intensive therapy and could be spared from the risk of increased toxicity. This consideration is particularly relevant in HNC where standard treatment often eradicates disease but with very high cost, including severe and long-lasting mucositis, chronic xerostomia, dental disease, and long-term swallowing dysfunction. These considerations are more critical with the increasing incidence of HPV-related HNCs as investigators actively attempt to design and test deintensified treatment regimens for this improved prognostic patient population.

Kim and colleagues used pretreatment DCE-MRI in 33 patients with HNC to evaluate response to CRT. Pretreatment K^{trans} values were 3-fold higher in complete responders than in partial responders ($P = 0.001$; ref. 36). The current study, with its longer term follow-up, showed similarly higher baseline K^{trans} levels in primary tumors and lymph nodes from patients without subsequent disease recurrence, a more robust clinical endpoint than response. Moreover, these findings suggest that pretreatment K^{trans}

could provide prognostic information independent from conventional Response Evaluation Criteria in Solid Tumors (RECIST) given that nearly all patients in the study had a CR at the primary site.

K^{trans} represents the vascular transfer coefficient and reflects vascular permeability as contrast moves out of the vasculature and into the interstitium. Permeability and perfusion closely approximate one another in an untreated tumor (16). Lyng and colleagues conducted immunohistochemical analysis of uterine cervix squamous carcinoma and showed that patients whose tumors had high vascular density (a surrogate for perfusion) had better oxygenated tumors and better prognosis than those with low vascular density (37). The powerful adverse influence of tumor hypoxia on treatment outcome in HNC is well known (3). The association of higher baseline K^{trans} values with a more favorable prognosis supports the concept of better perfusion being a favorable prognostic parameter.

Hoskin and colleagues conducted second DCE-MRIs after completion of accelerated RT in 12 patients with HNC and compared them with pretreatment studies (38). They assessed the maximum signal enhancement (E) in a primary tumor or lymph node. Mean ($\pm$SD) baseline E decreased from 0.76 ± 0.09 to 0.67 ± 0.04 after treatment in patients who were disease-free but increases from 0.81 ($\pm$0.21) to 1.07 ($\pm$0.25) in patients who subsequently failed. Similarly, the time to maximum enhancement (T_{max}) decreased after treatment in patients who were rendered disease-free by treatment, but it increased in those who recurred, similar to the increase in K^{trans} in our trial. Both E and T_{max} are dependent upon K^{trans} and would therefore be expected to move in step with this parameter (23).

Performance of serial scans at early and predetermined times during therapy is a unique aspect of the current trial. Comparison of pre versus posttreatment FMI parameters precludes modification of therapy based upon detection of adverse signals early during therapy. Early treatment-induced changes in K^{trans} could be useful for real-time assessment of therapeutic efficacy.

Wedam and colleagues treated 21 patients with locally advanced/inflammatory breast cancer using a combination of bevacizumab and cytotoxic chemotherapy. Four MRIs were conducted: at baseline and after cycles 1, 4, and 7. They showed a 75% decrease in K^{trans} over the course of treatment but did not detect a difference between responders and nonresponders (20). Hayes and colleagues conducted DCE-MRIs on 15 patients with breast cancer before and after their first of 6 cycles of multiagent chemotherapy. Responders had higher baseline K^{trans} values, which diminished after chemotherapy compared with nonresponders whose lower baseline K^{trans} values increased (39). The overall patterns and changes in K^{trans} in their study were similar to those in our trial.

The association between treatment-induced reductions in K^{trans} and favorable outcomes seems paradoxical. However, these changes may reflect reductions in vascular permeability rather than perfusion, especially in the context of agents such as bevacizumab. Reductions in vascular permeability during treatment lead to reductions in IFP (40). Elevated IFP is strongly correlated with greater risks of both local and distant recurrence in uterine cervix cancer independent of stage (41). Treatment-induced reductions in IFP would be expected to change hydrostatic gradients leading to net improvements in functional perfusion. Thus, treatment-induced reduction in K^{trans} may reflect a net improvement in perfusion.

Caution must be exercised in the interpretation of the data from the current study. Only 5 relapses were observed in the study population, making statistical testing unreliable. Consequently, we did not compute P values. The differences in baseline and temporal changes in K^{trans} between patients who did and did not recur must therefore be viewed as hypothesis generating. We believe that these apparent imaging differences are of sufficient clinical interest, however, to merit further investigation, especially given their correlation with a long-term endpoint rather than acute response to therapy.

Imaging of static anatomic parameters, such as tumor size, creates the tendency to attribute any subsequent changes to the intervening treatment. FMI measures dynamic physiologic processes subject to temporal fluctuations in the absence of any treatment, however. Therefore, treatment-induced changes in FMI parameters need to be interpreted with an understanding of the intrinsic temporal variability inherent to the tumors and/or normal tissues under investigation (42). Double baseline pretreatment positron emission tomography studies show significant day-to-day variation in tumor oxygenation in up to 30% of patients with HNC (43). Glucose metabolism may also fluctuate by 30% to 40% on a daily basis (44). Therefore, the intrinsic variability of K^{trans}, unknown for cancers in general and HNC in particular, constitutes a major focus of our present research.

Conclusions

The current study shows acceptable safety and encouraging efficacy with the integration of dual EGFR and VEGF inhibitors with CRT in locally advanced nonmetastatic HNC. The increased incidence of osteoradionecrosis and soft tissue necrosis may be associated with the use of bevacizumab. These results warrant further study in a larger multi-institutional and/or randomized setting. Identification of robust prognostic and predictive biomarkers may allow for more rational selection of patient populations who would benefit most from the addition of molecular targeted therapy. Using DCE-MRI to measure pretreatment K^{trans} and changes in K^{trans} early in the course of treatment may prospectively identify patients with HNC at high risk of treatment failure. Validation in a larger population could facilitate use of this tool to select or modify treatment strategies for individual patients.

Disclosure of Potential Conflicts of Interest

N.E. Ready is consultant/advisory board member for Genentech and has <$5,000 advisory role with Genentech. No potential conflicts of interest were disclosed by other authors.

Acknowledgments

Investigational agents were supplied by Genentech.

Grant Support

Budgetary support was provided by Genentech.

The costs of publication of this article were defrayed in part by the payment of page charges. This article must therefore be hereby marked *advertisement* in accordance with 18 U.S.C. Section 1734 solely to indicate this fact.

Received August 2, 2011; revised December 15, 2011; accepted January 2, 2012; published OnlineFirst January 17, 2012.

References

1. Jemal A, Siegel R, Xu J, Ward E. Cancer statistics, 2010. CA Cancer J Clin 2010;60:277–300.
2. Pignon JP, le Maitre A, Maillard E, Bourhis J. Meta-analysis of chemotherapy in head and neck cancer (MACH-NC): an update on 93 randomised trials and 17,346 patients. Radiother Oncol 2009;92:4–14.
3. Brizel DM, Dodge RK, Clough RW, Dewhirst MW. Oxygenation of head and neck cancer: changes during radiotherapy and impact on treatment outcome. Radiother Oncol 1999;53:113–7.
4. Ferrara N. VEGF as a therapeutic target in cancer. Oncology 2005;69 Suppl 3:11–6.
5. Onesto C, Hannoun-Levi JM, Chamorey E, Formento JL, Ramaioli A, Pages G. Vascular endothelial growth factor-A and Poly(A) binding protein-interacting protein 2 expression in human head and neck carcinomas: correlation and prognostic significance. Br J Cancer 2006;94:1516–23.
6. O-charoenrat P, Rhys-Evans P, Eccles SA. Expression of vascular endothelial growth factor family members in head and neck squamous cell carcinoma correlates with lymph node metastasis. Cancer 2001; 92:556–68.
7. Dings RP, Loren M, Heun H, McNiel E, Griffioen AW, Mayo KH, et al. Scheduling of radiation with angiogenesis inhibitors anginex and Avastin improves therapeutic outcome via vessel normalization. Clin Cancer Res 2007;13:3395–402.
8. Seiwert TY, Haraf DJ, Cohen EE, Stenson K, Witt ME, Dekker A, et al. Phase I study of bevacizumab added to fluorouracil- and hydroxyurea-based concomitant chemoradiotherapy for poor-prognosis head and neck cancer. J Clin Oncol 2008;26:1732–41.
9. Ang KK, Berkey BA, Tu X, Zhang HZ, Katz R, Hammond EH, et al. Impact of epidermal growth factor receptor expression on survival and pattern of relapse in patients with advanced head and neck carcinoma. Cancer Res 2002;62:7350–6.
10. Bonner JA, Harari PM, Giralt J, Azarnia N, Shin DM, Cohen RB, et al. Radiotherapy plus cetuximab for squamous-cell carcinoma of the head and neck. N Engl J Med 2006;354:567–78.
11. Cohen EE. Role of epidermal growth factor receptor pathway-targeted therapy in patients with recurrent and/or metastatic squamous cell carcinoma of the head and neck. J Clin Oncol 2006;24:2659–65.
12. Vermorken JB, Mesia R, Rivera F, Remenar E, Kawecki A, Rottey S, et al. Platinum-based chemotherapy plus cetuximab in head and neck cancer. N Engl J Med 2008;359:1116–27.
13. Benavente S, Huang S, Armstrong EA, Chi A, Hsu KT, Wheeler DL, et al. Establishment and characterization of a model of acquired resistance to epidermal growth factor receptor targeting agents in human cancer cells. Clin Cancer Res 2009;15:1585–92.
14. Bozec A, Formento P, Lassalle S, Lippens C, Hofman P, Milano G. Dual inhibition of EGFR and VEGFR pathways in combination with irradiation: antitumour supra-additive effects on human head and neck cancer xenografts. Br J Cancer 2007;97:65–72.
15. Cohen EE, Davis DW, Karrison TG, Seiwert TY, Wong SJ, Nattam S, et al. Erlotinib and bevacizumab in patients with recurrent or metastatic squamous-cell carcinoma of the head and neck: a phase I/II study. Lancet Oncol 2009;10:247–57.
16. Tofts PS, Brix G, Buckley DL, Evelhoch JL, Henderson E, Knopp MV, et al. Estimating kinetic parameters from dynamic contrast-enhanced T(1)-weighted MRI of a diffusable tracer: standardized quantities and symbols. J Magn Reson Imaging 1999;10:223–32.
17. Cooper RA, Carrington BM, Loncaster JA, Todd SM, Davidson SE, Logue JP, et al. Tumour oxygenation levels correlate with dynamic contrast-enhanced magnetic resonance imaging parameters in carcinoma of the cervix. Radiother Oncol 2000;57:53–9.
18. George ML, Dzik-Jurasz AS, Padhani AR, Brown G, Tait DM, Eccles SA, et al. Non-invasive methods of assessing angiogenesis and their value in predicting response to treatment in colorectal cancer. Br J Surg 2001;88:1628–36.
19. Stomper PC, Winston JS, Herman S, Klippenstein DL, Arredondo MA, Blumenson LE. Angiogenesis and dynamic MR imaging gadolinium enhancement of malignant and benign breast lesions. Breast Cancer Res Treat 1997;45:39–46.
20. Wedam SB, Low JA, Yang SX, Chow CK, Choyke P, Danforth D, et al. Antiangiogenic and antitumor effects of bevacizumab in patients with inflammatory and locally advanced breast cancer. J Clin Oncol 2006; 24:769–77.
21. Tomura N, Omachi K, Sakuma I, Takahashi S, Izumi J, Watanabe O, et al. Dynamic contrast-enhanced magnetic resonance imaging in radiotherapeutic efficacy in the head and neck tumors. Am J Otolaryngol 2005;26:163–7.
22. Craciunescu O, Brizel D, Cleland E, Yoo D, Muradyan N, Carroll M, et al. Dynamic contrast enhanced-MRI in head and neck cancer patients: variability of the precontrast longitudinal relaxation time (T10). Med Phys 2010;37:2683–92.
23. Tofts PS, Berkowitz B, Schnall MD. Quantitative analysis of dynamic Gd-DTPA enhancement in breast tumors using a permeability model. Magn Reson Med 1995;33:564–8.
24. Trotti A, Bellm LA, Epstein JB, Frame D, Fuchs HJ, Gwede CK, et al. Mucositis incidence, severity and associated outcomes in patients with head and neck cancer receiving radiotherapy with or without chemotherapy: a systematic literature review. Radiother Oncol 2003; 66:253–62.
25. Garden AS, Harris J, Trotti A, Jones CU, Carrascosa L, Cheng JD, et al. Long-term results of concomitant boost radiation plus concurrent cisplatin for advanced head and neck carcinomas: a phase II trial of the radiation therapy oncology group (RTOG 99-14). Int J Radiat Oncol Biol Phys 2008;71:1351–5.
26. Salama JK, Haraf DJ, Stenson KM, Blair EA, Witt ME, Williams R, et al. A randomized phase II study of 5-fluorouracil, hydroxyurea, and twice-daily radiotherapy compared with bevacizumab plus 5-fluorouracil, hydroxyurea, and twice-daily radiotherapy for intermediate-stage and T4N0-1 head and neck cancers. Ann Oncol 2011;22:2304–9.
27. Brizel DM, Albers ME, Fisher SR, Scher RL, Richtsmeier WJ, Hars V, et al. Hyperfractionated irradiation with or without concurrent chemotherapy for locally advanced head and neck cancer. N Engl J Med 1998;338:1798–804.
28. Ang KK, Harris J, Wheeler R, Weber R, Rosenthal DI, Nguyen-Tan PF, et al. Human papillomavirus and survival of patients with oropharyngeal cancer. N Engl J Med 2010;363:24–35.
29. Ang KK, Zhang QE, Rosenthal DI, Nguyen-Tan P, Sherman EJ, Weber RS, et al. A randomized phase III trial (RTOG 0522) of concurrent accelerated radiation plus cisplatin with or without cetuximab for stage III-IV head and neck squamous cell carcinomas (HNC). J Clin Oncol 29: 2011 (suppl; abstr 5500).
30. Chen LF, Cohen EE, Grandis JR. New strategies in head and neck cancer: understanding resistance to epidermal growth factor receptor inhibitors. Clin Cancer Res 2010;16:2489–95.
31. Ko AH, Venook AP, Bergsland EK, Kelley RK, Korn WM, Dito E, et al. A phase II study of bevacizumab plus erlotinib for gemcitabine-refractory metastatic pancreatic cancer. Cancer Chemother Pharmacol 2010;66: 1051–7.
32. Tol J, Koopman M, Cats A, Rodenburg CJ, Creemers GJ, Schrama JG, et al. Chemotherapy, bevacizumab, and cetuximab in metastatic colorectal cancer. N Engl J Med 2009;360:563–72.

33. Van Cutsem E, Kohne CH, Hitre E, Zaluski J, Chang Chien CR, Makhson A, et al. Cetuximab and chemotherapy as initial treatment for metastatic colorectal cancer. N Engl J Med 2009;360:1408–17.
34. Cohen EE, Haraf DJ, Kunnavakkam R, Stenson KM, Blair EA, Brockstein B, et al. Epidermal growth factor receptor inhibitor gefitinib added to chemoradiotherapy in locally advanced head and neck cancer. J Clin Oncol 2010;28:3336–43.
35. Soulieres D, Senzer NN, Vokes EE, Hidalgo M, Agarwala SS, Siu LL. Multicenter phase II study of erlotinib, an oral epidermal growth factor receptor tyrosine kinase inhibitor, in patients with recurrent or metastatic squamous cell cancer of the head and neck. J Clin Oncol 2004;22:77–85.
36. Kim S, Loevner LA, Quon H, Kilger A, Sherman E, Weinstein G, et al. Prediction of response to chemoradiation therapy in squamous cell carcinomas of the head and neck using dynamic contrast-enhanced MR imaging. AJNR Am J Neuroradiol 2010;31:262–8.
37. Lyng H, Sundfor K, Rofstad EK. Oxygen tension in human tumours measured with polarographic needle electrodes and its relationship to vascular density, necrosis and hypoxia. Radiother Oncol 1997;44:163–9.
38. Hoskin PJ, Saunders MI, Goodchild K, Powell ME, Taylor NJ, Baddeley H. Dynamic contrast enhanced magnetic resonance scanning as a predictor of response to accelerated radiotherapy for advanced head and neck cancer. Br J Radiol 1999;72:1093–8.
39. Hayes C, Padhani AR, Leach MO. Assessing changes in tumour vascular function using dynamic contrast-enhanced magnetic resonance imaging. NMR Biomed 2002;15:154–63.
40. Willett CG, Boucher Y, di Tomaso E, Duda DG, Munn LL, Tong RT, et al. Direct evidence that the VEGF-specific antibody bevacizumab has antivascular effects in human rectal cancer. Nat Med 2004;10:145–7.
41. Milosevic M, Fyles A, Hedley D, Pintilie M, Levin W, Manchul L, et al. Interstitial fluid pressure predicts survival in patients with cervix cancer independent of clinical prognostic factors and tumor oxygen measurements. Cancer Res 2001;61:6400–5.
42. Brizel DM, Rosner GL, Prosnitz LR, Dewhirst MW. Patterns and variability of tumor oxygenation in human soft tissue sarcomas, cervical carcinomas, and lymph node metastases. Int J Radiat Oncol Biol Phys 1995;32:1121–5.
43. Fakhry C, Westra WH, Li S, Cmelak A, Ridge JA, Pinto H, et al. Improved survival of patients with human papillomavirus-positive head and neck squamous cell carcinoma in a prospective clinical trial. J Natl Cancer Inst 2008;100:261–9.
44. Velasquez LM, Boellaard R, Kollia G, Hayes W, Hoekstra OS, Lammertsma AA, et al. Repeatability of 18F-FDG PET in a multicenter phase I study of patients with advanced gastrointestinal malignancies. J Nucl Med 2009;50:1646–54.